# THREE-DIMENSIONAL STRUCTURE OF THE CENTRAL MITOTIC SPINDLE OF *DIATOMA VULGARE*

J. RICHARD McINTOSH, KENT L. McDONALD, M. KAYE EDWARDS, and B. M. ROSS

From the Department of Molecular, Cellular and Developmental Biology, University of Colorado, Boulder, Colorado 80309

ABSTRACT

Central mitotic spindles in *Diatoma vulgare* have been investigated using serial sections and electron microscopy. Spindles at both early stages (before metaphase) and later stages of mitosis (metaphase to telophase) have been analyzed. We have used computer graphics technology to facilitate the analysis and to produce stereo images of the central spindle reconstructed in three dimensions. We find that at prometaphase, when the nuclear envelope is disassembling, the spindle is constructed from two sets of polar microtubules (MTs) that interdigitate to form a zone of overlap. As the chromosomes become organized into the metaphase configuration, the polar MTs, the spindle, and the zone of overlap all elongate, while the number of MTs in the central spindle decreases from >700 to ~250. Most of the tubules lost are short ones that reside near the spindle poles. The previously described decrease in the length of the zone of overlap during anaphase central spindle elongation is clearly demonstrated in stereo images. In addition, we have used our three-dimensional data to determine the lengths of the spindle MTs at various times during mitosis. The distribution of lengths is bimodal during prometaphase, but the short tubules disappear and the long tubules elongate as mitosis proceeds. The distributions of MT lengths are compared to the length distributions of MTs polymerized in vitro, and a model is presented to account for our findings about both MT length changes and microtubule movements.

KEY WORDS mitosis · microtubules · computer analysis · three-dimensional reconstruction · diatom · central spindle

Much of the physiological research that has been done on mitosis has employed a rather small group of cell types which have become justly famous through their suitability for a particular kind of investigation, for example, microbeam irradiation or chromosome micromanipulation. EM studies of these organisms have been carried out, and some quantitative information about their spindle fine structure is available (reviewed in references 3 and 7). In general, though, the cells suitable for detailed physiology and elegant light microscope study have been difficult to examine thoroughly with the EM, because their spindles are 6–50 μm in length and display 600–5,000 microtubules (MTs) in a single cross section.

Over the past few years, studies on the fine structure of mitosis in a wide variety of lower eukaryotic cells have been published (reviewed in references 8, 11, 17, and 30). These studies have shown that the spindles of some fungi and algae



J. CELL BIOLOGY © The Rockefeller University Press · 0021-9525/79/11/0428/15 $1.00
Volume 83 November 1979 428–442

are aptly suited for detailed study with the EM, because the spindles are small, contain only a few MTs, and are comparatively well ordered. Unfortunately, it will be difficult to get detailed physiological information about these cells, just because they are so small. One is therefore in a technical dilemma as to how to carry out a thorough, wide-ranging study of spindle structure and physiology in any single cell. One would like to develop methods that would give high resolution structural detail of the larger, experimentally accessible spindles.

There are at least three ways in which this might be done. One is to use the data from serial sections to make static, mechanical models of mitotic spindles—a thorough but cumbersome approach. A second, more feasible solution is high voltage electron microscopy (HVEM) of whole isolated spindles or thick sections of spindles. The available data on HVEM of large spindles (2, 5, 18, 19, 21, 22) show, however, that there is so much complexity in the images that quantitation, e.g., plotting the course of every MT, is an essentially impossible task. With small spindles, the HVEM has been more successful. The study by Peterson and Ris (28) is one of the most complete quantitative studies of mitosis on any organism; yet, even with this spindle, it is difficult to follow individual MTs along their entire length and to resolve their ends at the spindle poles. The final option for realizing total spindle structure at high resolution is to analyze and reconstruct spindles from serial sections using computer graphics technology. The validity and usefulness of this approach for studying the distribution of cells in organisms or tissues (10, 12, 31, 39, 40), or of organelles within cells (27, 34), is well established. We have already shown (21, 22) that this kind of analysis can also be applied to spindle structure studies, but there are special problems not encountered in whole cell or whole organism reconstructions. The problems are chiefly ones of maximizing resolution and minimizing distortion. Despite these difficulties, we have found that the approach is useful for analyzing and visualizing mitotic spindle structure.

In this paper and the one which follows (15), we have used computer graphics technology to help reconstruct the central spindle of *Diatoma vulgare* in three dimensions and have obtained data on the interaction of spindle tubules. We have selected *Diatoma* for the first investigation of this kind for several reasons: (*a*) the number of MTs in the spindle and the overall spindle dimensions are reasonable for a pilot study, (*b*) we had a body of serial section data already on hand, (*c*) we could use existing hand-tracking data (16) as a control for the accuracy of some aspects of the computer analysis, and (d) new information on prometaphase and early metaphase stages would allow us to extend the existing body of knowledge on the central spindle of this organism. This paper reports on spindle structure along the pole-to-pole axis at various stages of mitosis. In the next paper (15), we deal with the cross-sectional arrangement of the central spindle MTs. The prognosis for using computer graphics as an aid for the detailed structural study of bigger spindles is discussed.

## MATERIALS AND METHODS

*Diatoma vulgare* Bory was collected locally and fixed either with standard methods (29) or with a semi-simultaneous application of glutaraldehyde and osmium tetroxide (32, 36). The latter method gives better general cell preservation, but the MT components of the spindle structure as reflected in the length distributions and MT number distributions are the same with the two methods. Fixed mitotic cells were identified in thin wafers of Epon with the light microscope, selected, oriented, and serially sectioned as previously described (16). Sections were stained with uranyl acetate and lead citrate, and examined in a Philips 300 EM equipped with a goniometer stage. This stage allowed us to rotate successive sections about the optical axis so that they were in the same orientation relative to the photographic film, and to tilt each section to bring it into the best possible cross-sectional view. Pictures were taken at an instrument magnification of 35,000 on 3¼ × 4 inch film and photographically enlarged to a final maginfication of ~120,000.

The two-dimensional coordinates of each MT in the central spindle were digitized using a home-made, polar coordinate digitizer designed by Lee Peachey of the University of Pennsylvania (27). The reproducibility of the digitizer is within ±0.01 mm; its accuracy is within about ±0.1 mm. The reliability of stylus placement by the operator identifying the center of a microtubule is about ±0.3 mm, approximately one-tenth of a microtubule diameter at the magnification used. The positions of all the microtubules on one section were digitized, and their coordinates were printed onto paper tape. A second micrograph was then positioned on the digitizer so that its microtubules were approximately in register with the MTs on the first, and the process was repeated. Reiteration converted the entire structure of the central spindle to computer-compatible form.

The digitized positions of the central spindle MTs were placed on disc storage by a Control Data Corporation (CDC) 6400 at our University Computer Center. The microtubule positions could then be called up, sec-

tion-pair by section-pair, and displayed on the screen of a CDC 774 interactive graphics terminal driven by a CDC 1700 minicomputer and interfaced with a CDC 6400. In our system, the first section is displayed as a set of X's and the second as a set of O's, so the operator can distinguish the two data sets on the screen. At this time the set of points representing microtubule centers from the second section can be translated and rotated relative to the first set to achieve optimum alignment of the data from the two micrographs. If the specimen in the EM was tilted in passing from one section to the next, a uniaxial distortion of the data is now evident. This distortion can be temporarily removed by a transformation determined visually at the graphics terminal. When the data from the two sections are reasonably superposed, the operator calls up a computer-mediated tracking routine. The routine operates upon a fraction of the total spindle cross-section area at any one time, starting at the lower left-hand corner of the image and marking off a rectangle which will, on the average, contain 10 MTs from the first section. The computer asks whether there is a microtubule center in the second section lying with X and Y values less than 3/2 MT diameters away from each tubule center in this subset of the MTs in the first section. A two-dimensional vector is now drawn from each point in the subset of points from the first section to any point in the second section that lies within the trial search radius, and the average of all such connecting vectors is calculated. The two pictures are then translated by the negative of this average vector to improve the local alignment. Each MT in the subset of the first section is again compared against those on the second section to ask whether a tubule now lies within a distance of one MT diameter. Correspondences identified at this second scan are stored. The routine now redefines the area of search to include half the old tubules and half new tubules, and the process is reiterated until the entire cross-section area has been scanned. Tracking MTs in this way takes the computer ~5 s for 100 tubule pairs.

At the end of the tracking process, the data from the two sections are again displayed as X's and O's, with any points identified as successive positions along the same MT now linked by a line segment. MT positions identified as either an X or an O which have no match blink to attract the attention of the operator. The matches are then checked against the original micrographs to make sure that there are no digitizing errors or incorrect matches. To aid in this check, the sections preceding and following the two sections already visible can be displayed on the screen using different symbols. They too can be aligned relative to the existing sections in order that one may track by eye over a greater MT length than a single section pair. When the operator is satisfied with the correspondences displayed upon the screen, they are stored in memory, and he proceeds to the next section pair, so MT positions on the section displayed as O's in the correspondences just determined now become X's and the MTs of the new section are displayed as O's. Any transformations made to facilitate determination of correspondences at the interactive graphics terminal are erased as the operator proceeds, so the original digitized data are always used in final determinations of spindle structure. The tracking process is reiterated until one has processed all pairs of adjacent sections.

Each two-dimensional point marking an MT in a section is now regarded as a three-dimensional point, using section number as the coordinate along the spindle axis. The collection of three-dimensional points corresponding to one MT can now be handled as a set. For example, those sets representing MT with one end in the vicinity of a pole can be identified and ordered by microtubule length for display. At this time, we calculate histograms of MT number vs. position along the spindle axis, various properties of the cross-sectional MT density distribution, and other useful displays for spindle analysis. The three-dimensional points along each MT are also used to calculate two-dimensional projections of the three-dimensional structure onto any chosen plane. Fig. 1 shows a small region of such a projection from an anaphase spindle. It is clear that the reconstruction contains lines with sufficiently sharp bends that they do not closely resemble spindle MTs in longitudinal orientation. These bends are caused by natural curvature of the MTs, by electron optical and printing distortions, by small digitizing errors, and most importantly, by variation in the projection of the sections resulting from tilt in the goniometer stage during microscopy. To facilitate viewing of these complex images, we have smoothed the curves representing each MT by using a polynomial of chosen order fitted by the method of least squares to the points that represent each tubule. The programs allow the operator to select the order of this polynomial, but we have found that fourth-order functions serve the purpose well. Fig. 2 is a fourth-order smoothing of the same data displayed in Fig. 1. The output from this

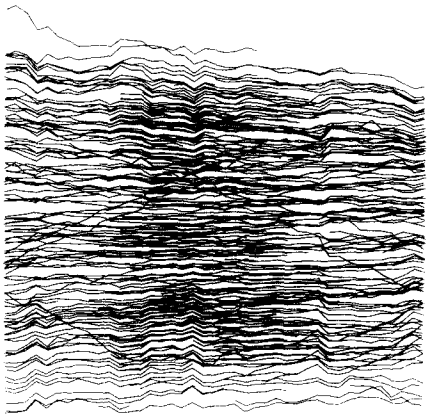

FIGURE 1 MT linkages in a region of the anaphase 1 spindle before a curve-fitting polynomial is applied.

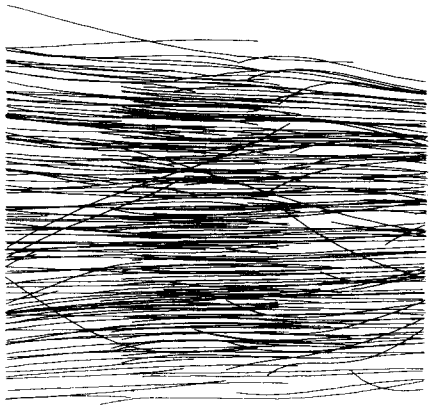

FIGURE 2 The same region after curve-fitting with a fourth-order polynomial.

three-dimensional reconstruction is either a microfilm display of the relevant graphs and histograms or a Calcomp Plotter drawing of the two-dimensional projection of the full spindle structure. We have used standard stereo projection methods to generate two similar pictures of each spindle in order to allow stereo viewing, and thus to obtain a sense of the three-dimensional architecture of the reconstructed spindle.

While our reconstructions of the spindle represent a step forward in the completeness and ease of spindle structure analysis, there are limitations to our current methods which must be made clear. We now know that one should determine the relationship between a known structure and its image in the EM at the magnification chosen for work, and determine how this relationship changes at different angles of specimen tilt and different heights, using different objective lens currents to bring the specimen into accurate focus. It would then be possible to devise a digital transformation to normalize all micrographs and remove the several electron optical and tilting distortions by computation. It will be seen, upon careful viewing of our three-dimensional reconstructions, that we have included a certain amount of distortion by not removing the effects of variation in focus and tilt. Section thickness should be measured by quantitative electron microscopy at the time the original micrographs are obtained. We planned to measure section thickness with a quantitative interference microscope but found this method unreliable for thin sections placed on slot grids. The specimen support films on many of our grids were broken by the time we realized the importance of quantitative electron microscopy at low magnification for determining section thickness, so in this study we are unable to use a parameter more accurate than section number to describe position along the spindle axis.

The accuracy of this scaling factor is limited by the uniformity of section thickness. In effect, we are assuming that all our sections are of the same thickness. This assumption is justified by our finding that when the spindle size in a Calcomp drawing is defined by section number, i.e., all spindles are scaled such that a 40-section spindle is just half the length of an 80-section spindle. etc., the ratio of the spindle width in the drawing to its width on the original micrographs is constant from one spindle to the next to within 10%. Another way of checking the accuracy of section number as a parameter reflecting axial position is to see how the spindle lengths determined in cross section (section number) × (avg section thickness ~750 Å) agree with the lengths of other *Diatoma* spindles of equivalent stage in mitosis measured directly from longitudinal sections (Table I). Except for the telophase cell, the figures are in good agreement. It is possible that the telophase sections were thinner than 750 Å which would reduce both the spindle length and the length of the individual tubules reported here for that cell.

Early in our analysis we decided to use the eye of a biologist rather than some computer-mediated pattern recognition routine to identify the positons of the microtubules in cross section. We have had enough experience with unsuccessful attempts at automated tubule recognition to realize that this was a good decision. Another decision, namely to minimize hardware purchases, has led us to omit three potentially useful developments: the photogrammetric corrections of distortion mentioned above, a convenient comparison between the micrographs and the digitized data, and some sort of interactive quality control on the final structure of the spindle. The second and third of these jobs we have accomplished on the spindles shown here by more tedious methods acceptable in the current study. By omitting the first, we have concluded our study with slightly distorted final spindle structures. These distortions will be discussed below; we accept them for the moment since removing them will require major new software development. We hope to rebuild our programs over the next few years, incorporating the experience from this study and the improved graphics technology currently available.

TABLE I

*Comparison of Central Spindle Lengths as Determined from Longitudinal vs. Cross Sections*

| Stage | Length in longitudinal section | No. of longitudinal samples | Length in xs* (avg section = 750 Å thick) |
|---|---|---|---|
| | μm | | μm |
| Prometaphase | 3.00 | 2 | 3.50 |
| Metaphase | 5.25 | 5 | 5.25 |
| Anaphase | 6–7.0 | 5 | 6–7.2 |
| Telophase | 7–8.0 | 2 | 9.4 |

* Determined from the spindles used in the present study.

## RESULTS

When a mitotic spindle is cut into serial cross sections, structural details along the spindle axis are fragmented. The simplest form of reassembling the spindle is to plot the number of MTs per cross section against the section number along the spindle axis. Figs. 3 and 4 portray the central spindle of a prometaphase cell and a metaphase cell with this simple representation. Since the section number differs from Figs. 3 to 4, we infer that the metaphase spindle is longer than the prometaphase. The graphs demonstrate that the number of MTs per section at metaphase is less than at prometaphase. They also indicate a trend which can be followed through mitosis by comparing these data with previously published graphs of MT number vs. position for *Diatoma* (16). At prometaphase, the axial distribution of MT number shows three peaks: one central peak, and one near each pole. From prometaphase through anaphase the polar peaks decrease monotonically relative to the troughs. The central peak is comparatively stable through mitosis and approximately retains its height relative to the trough on either side until late anaphase or telophase (16).

By tracking MTs from one section to another it is possible to identify the section in which each tubule of a spindle begins and ends. Figs. 5 and 6 show the axial distributions of MT length and position for the prometaphase and metaphase cells shown in Figs. 3 and 4. Again, the abscissa of the graph is section number, reflecting position along the spindle axis. The ordinate of each graph has no geometrical significance with respect to the structure of the spindle. It does serve, however, to indicate the number of MTs in the spindle at different positions along the spindle axis. These graphs are slightly different from the comparable ones for *Diatoma* published previously because these two spindles contain too many MTs to be resolved as individual lines in a printable display of reasonable size. For these graphs all polar MTs (defined as MTs with one end on a pole, the other end free) of each half-spindle were ordered with respect to the position of their nonpolar ends along the spindle axis, and an envelope was drawn around the endings of the MTs. It is the envelope which is displayed. Fragment MTs (having neither end at a pole) or continuous MTs (with both ends at a pole) are displayed separately at the bottom of each graph. In prometaphase the whole central spindle contains 730 polar MTs (392 + 338 in the two half-spindles). In metaphase there are 526 polar MTs (255 + 271). These numbers are considerably higher than the values obtained for the

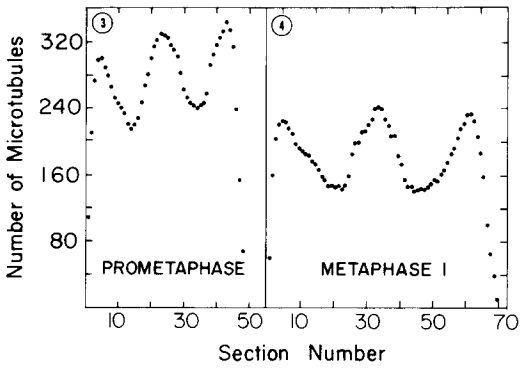


FIGURES 3 and 4 MT distribution profiles for central spindles in prometaphase (Fig. 3) and early metaphase (Fig. 4).

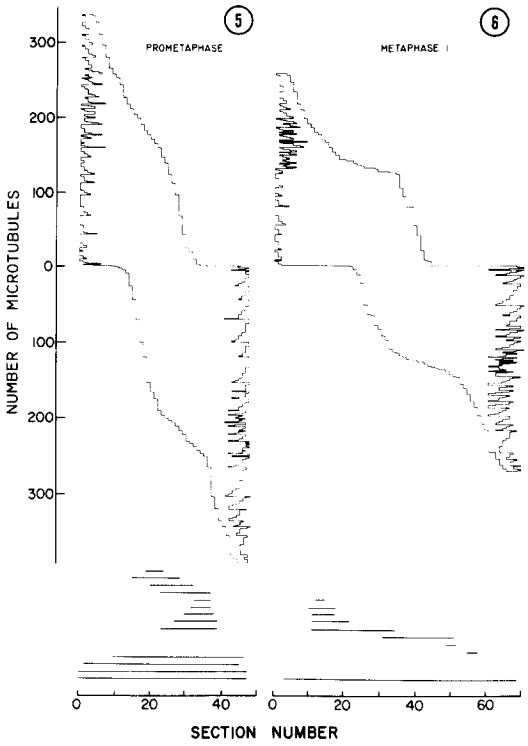


FIGURES 5 and 6 The distribution of MT ends for prometaphase (Fig. 5) and early metaphase (Fig. 6) spindles. The MTs are arranged along the spindle axis (=abscissa) according to their points of origin and termination. The ordinate serves to indicate the number of MTs in each spindle or half-spindle. The continuous MTs and free MTs and their points of origin and termination are shown at the bottom of each figure.

total polar MTs of the *Diatoma* spindles from later stages which range from 214 to 262 (16).

This distribution is convenient for studying the axial positions of MTs at various times during mitosis. Much geometrical information is lost, however, because the display is an intellectual construct rather than a physical representation of the full spindle. A more complete presentation of spindle structure is available as a result of the computer programs we have used in this study. Fig. 7 is a stereo projection of the MTs in the central spindle of the prometaphase cell previously shown in Figs. 3 and 5. The width and depth of the spindle are in accurate proportion in this projection, but the length (the vertical dimension) has been shortened by a factor of 2 to facilitate viewing. At first sight these images are formidably complex, but careful stereo viewing will permit interpretation of the spindle structure. Most tubules are seen to have one end near a pole. The polar regions contain many short tubules, accounting for the peaks in microtubule number seen at the spindle ends in Fig. 3. Stereo viewing reveals that the short tubules are approximately uniformly distributed over the cross-sectional area of the spindle pole. Many of the short tubules at the lower pole are curved and run for portions of their length at sharp angles with respect to the spindle axis. The curvatures of the short MTs on opposite sides of the spindle generally face one another. We interpret these highly curved tubules as artifacts of our reconstructions resulting from the changes in the section tilt and from the small number of points defining these curves. This interpretation is supported by the following four observations: (*a*) short, curved MTs are found along the spindle where sections were tilted in the EM to improve viewing; (*b*) the curvature is slight near the spindle axis and increases with increasing distance from the axis; (*c*) in the one spindle where no changes in section tilt angle were introduced, the curvatures of short tubules are much less; and (*d*) no such curved MTs are seen in longitudinal sections of *Diatoma* spindles (29).

The majority of the central spindle tubules with one end at a pole are long enough to extend into the mid-region of the spindle where they interdigitate with similar tubules from the opposite pole. We know from longitudinal sections of the *Diatoma* central spindle (29) that the tubules in the overlap region are mostly straight. Thus, the curvature and resulting oblique orientation of the MT ends in the region of overlap seen in Fig. 7 (and to a lesser extent in the remaining stereo images) are probably other artifacts of the curve-fitting routine. A few of the longer tubules with one end at a pole run obliquely to the spindle axis for their entire lengths. On account of the presence of corresponding oblique MT profiles in the cross sections, we are confident that these tubules are real. Note, however, that because of our shortening of the spindle, both the obliquity of these tubules and the curvatures cited above have been exaggerated.

Fig. 8 is a stereo projection of the metaphase spindle shown in Fig. 6. The length of this and all the other stereo pairs have been defined by the number of sections required to cut from one pole to the other, and then shortened by a factor of 2 to ease viewing.

The increase in spindle length from prometaphase to metaphase is readily seen by comparison of the two stereo images shown in Figs. 7 and 8. The decrease in total microtubule number is reflected in the decrease in spindle width with roughly constant tubule density in the spindle cross section. Microtubule density as a function of position along the spindle and of time in mitosis is considered quantitatively in the next paper (15). A comparison of the polar regions of Figs. 7–9 shows that the short tubules selectively disappear as mitosis progresses. The loss accounts for the disappearance of the peak in MT number seen near the poles in Figs. 3 and 4.

Looking at Figs. 7–9, one has the impression that the spindle becomes better ordered with time. This impression is due in part to the fact that the spindle shown in Fig. 9 was the one set of sections in which tilt did not have to be adjusted during microscopy of successive sections, so the artifact alluded to above is minimized. In addition, however, this spindle is apparently the best ordered of all the spindles we have studied: it contains few tubule fragments (as defined above), few oblique tubules, and the packing of the tubules appears uniform along the length of the spindle. In the following paper (15) we address ourselves to a quantitative determination of cross-sectional order that confirms this impression.

Figs. 10–12 show stereo projections of two anaphase spindles and a late anaphase-telophase spindle where stage has been determined by the position of the chromatin (data not shown). The images correspond to anaphase and telophase cells shown in Figs. 9, 10, and 12, respectively, of McDonald et al. (16). They show an increase in MT length as mitosis proceeds. The splitting of

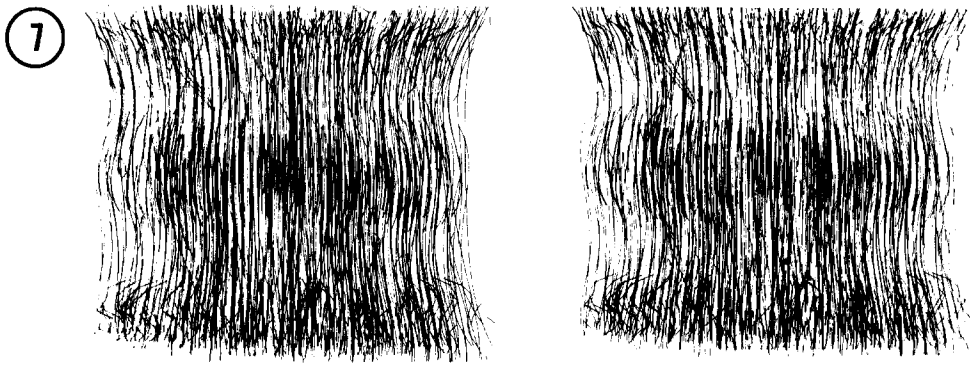


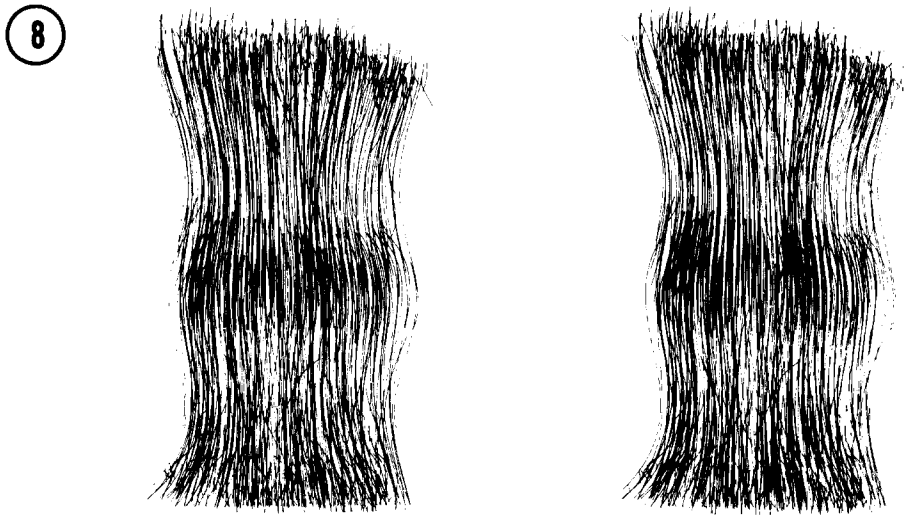


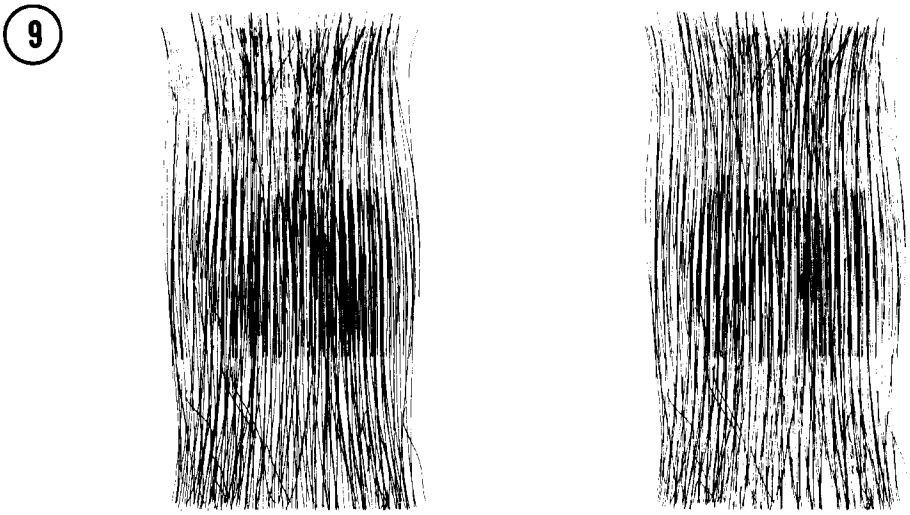


FIGURES 7–12 Stereo pairs of prometaphase (Fig. 7), early metaphase (Fig. 8), metaphase (Fig. 9), early anaphase (Fig. 10), late anaphase (Fig. 11), and telophase (Fig. 12) central spindles. Note the relatively large number of short MTs near the poles in Fig. 7. In Fig. 8, there are still some short MTs near the poles. In both cells these appear to be uniformly distributed at the pole, and not restricted to a particular region, e.g., the periphery. By metaphase (Fig. 9) and all later stages, the poles are no longer characterized by these short MTs. The prometaphase spindle (Fig. 7) is considerably wider than the other spindles. The half-spindle lengths appear to increase throughout mitosis. At telophase (Fig. 12), only the longest MTs overlap in the mid-region.

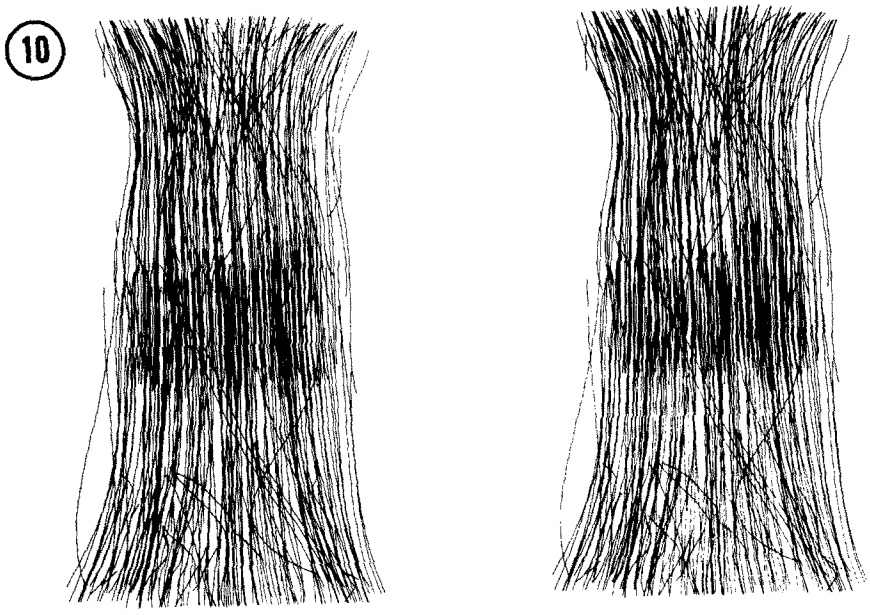
10

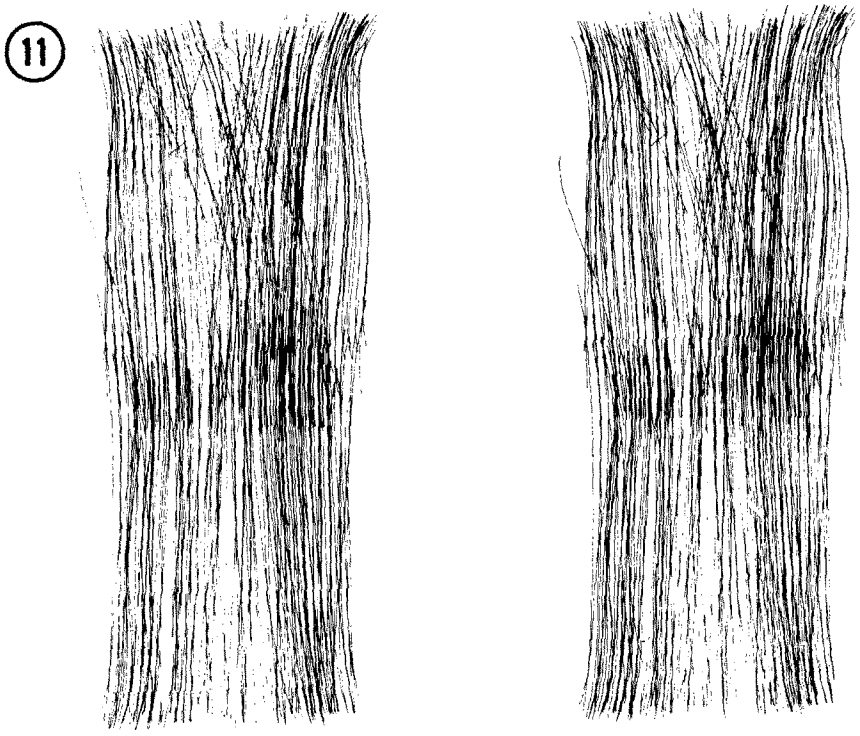
11

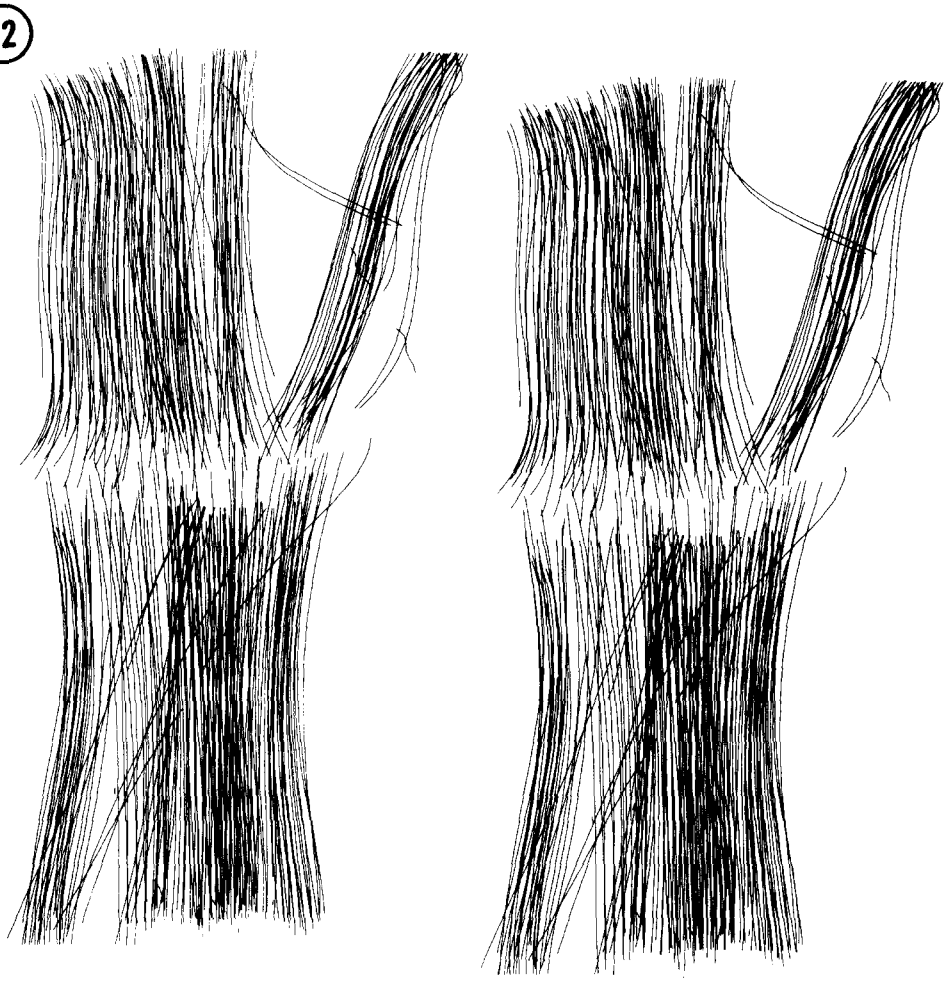


one-half of the central spindle at telophase into two bundles is actually in agreement with longitudinal views of a *Diatoma* spindle in late anaphase-telophase (29). All these reconstructions contain oblique tubules that wander across the spindle. Some of the wandering tubules have one end in the vicinity of a pole, while others are free in the sense that neither end is near a pole.

It is obvious from a comparison of these pictures that the length of the zone of overlap changes during the course of mitosis. The length of the zone may be defined quantitatively in two ways. By using the graphs of MT numbers vs. position along the spindle axis (e.g., Figs. 3 and 4), we can determine the width of the central peak or trough at half-height. This measure is dependable because the three-dimensional reconstructions allow us to be sure that there are few, if any, MT fragments in the region of overlap of polar tubules. We have determined the width at half-height by finding the section nearest to the peak on either side before the rise in number begins, finding the section at either edge of the peak where the distribution begins to level off, and using the corresponding ordinate values to determine a half-height on either side of the peak. Abscissa values for the half-heights were then determined by graphical interpolation. The difference between the abscissal positions of the half-heights on either side of the MT peak is one definition of the length of the zone of overlap (Table II). A second method for estimating the length of the zone of overlap is based on graphs such as those shown in Figs. 5 and 6. We fit a straight line to the region of the envelope marking the nonpolar ends of the longest polar tubules and extrapolated it to meet the hor-

TABLE II

*Changes in Length of the Zone of Overlap during Mitosis*

| Mitotic stage | Prometaphase | Early metaphase | Late metaphase | Early anaphase | Mid anaphase | Telophase |
|---|---|---|---|---|---|---|
| Length of the overlap at half height in sections | 10.7 | 13.1 | 22.2 | 17.0 | 13.0 | −9.5 |
| Extrapolated length in sections | 18.5 | 20.0 | 27.7 | 21.2 | 19.2 | 5.4 |
| Spindle length in sections | 48 | 70 | 69 | 80 | 96 | 125 |

izontal line that defines the boundary between the two half-spindles on the graphs. The distance on the abscissa between these two points of intersection is a second definition of the length of the zone of overlap (Table II). This method is the preferred one, because the structure of the telophase zone of overlap shows that the longest polar MTs are the ones that define the final length of the zone. Our data show that the zone of overlap tends to increase from prometaphase to metaphase and then decreases markedly during anaphase.

Table II shows that the change in length of the zone of overlap during anaphase (approx. 31 or 22 sections depending on definition) is not of sufficient magnitude to account for the anaphase increase in spindle length (56 sections). It appears from the stereo pictures that the microtubules themselves elongate. We have studied this elongation by determining the distribution of microtubule lengths in each of these spindles: Fig. 13 presents these data. The length of a microtubule has been approximated by the number of sections through which it runs. This approximation was deemed adequate because the real contour length of the MTs, as determined by summing the three-dimensional distances between the successive points along a tubule, is greater than the length determined by section number by only a few percent in almost all cases. The error intrinsic to our use of section number as a paraxial position coordinate exceeds the error introduced by neglecting MT obliquity. At prometaphase there are two major peaks in the distribution, one at short MT length and one at about 28 sections. As mitosis proceeds, the peak of short MTs dramatically decreases while the peak of longer tubules remains approximately constant in area and increases slightly in breadth as its mode moves to a greater mean length. The total amount of MT polymer in the central spindle as calculated by summing all MT lengths varies with time in mitosis as shown in Fig. 14.

## DISCUSSION

The computer graphics technology employed in this study has made it possible to get a new look at the central spindle of *Diatoma* in which EM resolution is combined with holistic perspective. The stereo projections of the total three-dimensional structure of the central spindle are complex, but comprehensible, because of the abstraction of each MT into a single curved line. The drawings presented here are not ideal, but they are a step forward in the determination and portrayal of spindle structure.

The greatest strength of the computer-facilitated approach does not, however, lie simply in the vivid display of qualitative features of the spindle; the computational power of the tools used makes possible certain steps in data processing that would be essentially impossible with any other approach. The validity of this statement is based more upon the material of the following paper than of this one, but the determination of the MT length distribution curves supports our contention.

There is, in principle, no upper bound to the numbers or lengths of MTs that could be handled with our approach. There are, however, practical limits that should be realized. Digitization of tubule position takes a few seconds for every tubule cross section, and total time increases linearly with the numbers of tubules and sections. Computer tracing of tubules from section to section requires several routines that employ matrix multiplication, so the requisite computer time, and hence cost, go as the square of the number of tubules per section. Further, the size and quality of the graphics terminal limit the number of tubules that may reasonably be displayed in any single cross section. We handled no more than 200 tubules per section as a data set, and have thus had to invent methods to put together two or more subsets of data to reconstruct the whole spindle of some *Diatoma* cells. Reconstruction of a larger spindle, such as

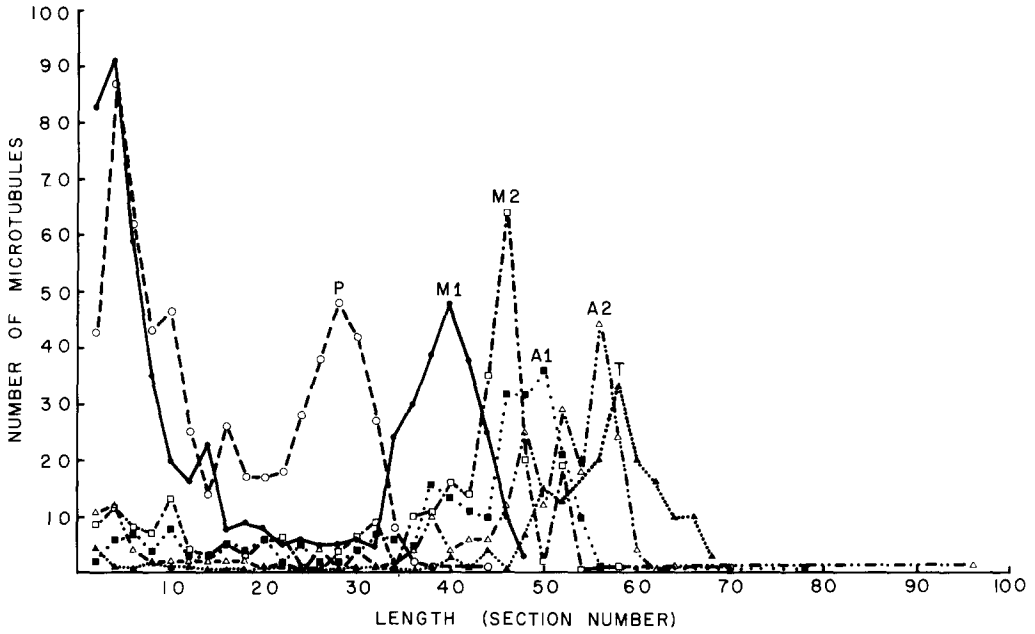


FIGURE 13 The distribution of microtubule lengths in half-spindles at prometaphase (*P*), early metaphase (*M1*), metaphase (*M2*), anaphase (*A1* and *A2*), and telophase (*T*).

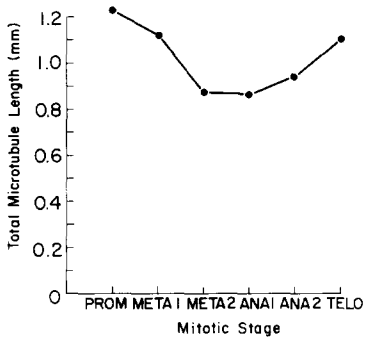


FIGURE 14 Total polymerized MT protein in spindles at prometaphase through telophase.

that of a mammalian cell, will require a similar trick unless more extensive facilities and more modest computer cost schedules are employed. Nonetheless, we are encouraged by our current results to go on to study not only other simple cells, but more complex ones as well.

We have used the four cells from this investigation which were also part of a previous study of *Diatoma* spindles (16) to assess the relative validity of the two methods for three-dimensional reconstruction. For two cells (Meta II and Telo) the correspondences were exact. For the other two (Ana I and II) there were a few disagreements in the sense that individual correspondences of one tubule from one section to the next were different. In each case, we found upon reexamination that we preferred the computer-facilitated correspondence. This is not because of some computer magic. All correspondences were ultimately established by eye; we are only using the computer as a bookkeeper. Tracking 100 MTs through 100 sections means 10,000 correspondences which is extremely tedious. The computer eases the work load by allowing the biologist to concentrate on the more difficult jobs, such as identifying the better of two similar matches. The easy correspondences are done automatically, and the bookkeeping requires no attention, so the quality of the final product is bound to be better.

The stereo images of the *Diatoma* spindle allow us to see new features in the formation of spindle structure. The development from prometaphase to metaphase involves increases in spindle length, in the length of the zone of overlap, and in the average length of the long spindle tubules. There is a decrease in the length of the short tubules, in the number of tubules, particularly the short ones, and in spindle width and depth. These observations imply that some long MTs are sufficiently stable to persist and elongate while all the short MTs and some long ones disappear. We would

like to understand not only this enigma, but the very existence of the short polar MTs which have not previously been described.

To provide a context in which to see these phenomena, let us look at the early stages of spindle formation in *Diatoma*. Spindle formation begins during prophase. Before prophase, a persistent polar complex is visible in the cytoplasm (29). It resembles the material of the spindle poles, but contains no obvious MTs. The complex is built from parallel plates that become the spindle poles with some structured, osmiophilic material in between. During prophase, MTs appear in this osmiophilic material, oriented approximately perpendicular to the plates and appearing to run from plate to plate. As prophase proceeds, these MTs elongate, the plates move apart, the plates enlarge in area, and the number of MTs increases. Recent data from *Fragilaria* (32), a diatom with a particularly small spindle, show that during this prophase growth all the spindle MTs run essentially from pole to pole; the images of prophase *Diatoma* spindles are completely consistent with this view. Sometime at about the onset of prometaphase when the nuclear envelope breaks down, the spindle structure changes drastically to yield the prometaphase structure we show here. Tippit et al. (37), in their study of *Fragilaria*, infer that the two half-spindles slide apart at the prophase to prometaphase transition, but stop sliding as the chromosomes attach to the central spindle. This view is consistent with everything we know, and seems entirely plausible as a mechanism in *Diatoma* as well.

With these facts in mind, we can interpret our observations of *Diatoma* spindle structure. Spindle growth begins in the cytoplasm when the two plates of the persistent polar complex are close. As the tubules grow, the plates move apart (Fig. 15). It is unlikely, however, that MT polymerization alone can account for the stages of spindle formation depicted in Fig. 15 *A* and *B*; some form of MT sliding is probable. This conclusion derives from the observation that in vitro MTs add subunits at their ends (4, 9) and a growing MT always adds subunits faster at one end then the other (1, 6). If MTs in vivo behave the same way, and if the MTs originating from the two poles are equivalent, then the MTs from each pole must slide past one another as they elongate. If both sliding and polymerization are occurring simultaneously, one cannot say a priori which is more likely to be the driving force for spindle elongation.

The transition from Fig. 15 *B* to *C* could be achieved by stopping the sliding of the MTs, and continuing to add subunits at the polar ends of the MTs. Alternatively, the sliding envisioned in early spindle formation could continue while the rate of polymerization decreased, giving rise to the transition from Fig. 15 *B* to *C*. In this model, subunit addition could occur at either tubule end, and the same result would follow. Regardless of which of these alternatives is correct, the transition will open up places on the polar plates that were previously occupied by the distal ends of MTs which butted against the pole opposite to the one that initiated them. These empty places are now exposed to a cytoplasm rich in polymerization-competent tubulin, and it is plausible that new MTs should initiate, thus accounting for both the presence of short MTs during prometaphase and the high density of MTs seen in the stereo pairs at the spindle poles (Fig. 15 *D*). This also explains why the short MTs are distributed all over the inward-facing surface of the polar plates rather than lying at the plate periphery where new (short) MTs might be expected to form.

Understanding our observation that the short MTs disappear with time in mitosis (Fig. 15 *E*) requires a different idea. It is well known from the study of MTs in a variety of cells that cross-bridged MTs tend to be more stable than MTs not cross-bridged (35, 38). It is also known that microtubule-associated proteins confer stability upon MTs in vitro by reducing the rate of MT disassembly (23). If we make the assumption, justified in the next paper, that MTs from either pole bridge to one another preferentially, then the disappearance of the short MTs while the longer ones are elongating is explained. The presumed interactions between the long polar MTs in the zone of overlap stabilize these tubules against disassembly, while the short MTs that cannot reach the zone of overlap after prometaphase, are comparatively unstable and disappear. We are suggesting that tubulin assem-

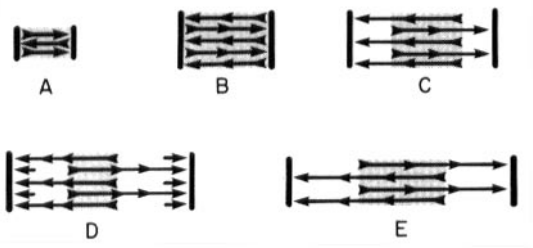


FIGURE 15 Hypothetical development of the central spindle through metaphase. See text for details.

bly can occur with different equilibria in neighboring regions of a cell as a result of geometrical considerations and the factors relating tubule stability to tubule interaction. An analogous idea has been suggested by Salmon (33) who proposes that stability is conferred upon certain spindle MTs by associating both of their ends with a microtubule-organizing center.

The pictures presented here, combined with previously published information on diatoms (16, 20, 37) show that the extent of overlapping of the interdigitating polar MTs decreases during anaphase. This change might occur by an active sliding of the two families of MTs relative to one another, or it might result from a disassembly of subunits from the nonpolar end of each MT with a contemporaneous addition of subunits at the polar end. Such "head-to-tail" polymerization of MTs has been described at steady state in vitro for neural MTs (13). These are not mutually exclusive concepts, and recent models of mitosis (14, 24) include both. It is clear from our data that some MT polymerization must occur during anaphase to obtain the observed increase in average MT length. We think it unlikely, however, that the polar assembly model accounts for the entire change in the zone of overlap, because this would require insertion of subunits between the pole and the MT that is pushing on it. In the sliding model, subunit addition can occur at the free MT end distal to the pole, a priori a more plausible suggestion. It should be emphasized that our data is inconsistent with a model which assumes that MT subunits add at the end distal to the pole but does not employ active MT sliding.

It is of interest to compare the distributions of MT lengths seen here with theoretical distributions of sizes for protein polymers and with empirical distributions found with polymerization of tubulin in vitro. The equilibrium distribution of lengths expected for a condensation polymerization reaction is a monotonic-decreasing negative exponential (26). If the system has not reached equilibrium but has arrived at a constant monomer concentration after assembly on spontaneously formed seeds, a Poisson distribution is expected (25). The observations concerning polymerization of neurotubulin in vivo are consistent with this latter prediction (6).

The bimodal distribution found in prometaphase and early metaphase *Diatoma* is unlike any other length distribution we have found reported for protein polymers. Our interpretation of the short tubules coming as a second wave of polymerization is helpful in reconciling this apparently unique distribution with what is generally known about polymer lengths. In this interpretation, the long tubules of prometaphase would be the result of the first wave of MT initiation occurring during prophase. If the initiation had been truly synchronous, a Gaussian distribution of lengths would be expected, and the symmetry of the long tubule peak at prometaphase is reasonably consistent with this view. The short tubule peak, which appears roughly Poisson in shape, is presumably caused by a second round of MT initiation, less synchronous than the first. These polymers may not have time for much elongation before conditions change and no longer favor polymerization and growth. The change in conditions could simply be the reduction in the monomer pool, or it could be something more subtle.

Table I shows that the sections used to prepare the telophase cell may have been thinner than the sections used for the other cells. If this is true, the peak describing telophase tubule distribution is too far to the right, but none of our major points is affected. Note that in "M2," "A1," and "A2," there are a very few MTs that are substantially longer than all the rest. These are the few continuous MTs previously described by McDonald et al. (16). Their anomalous appearance on this graph is further evidence for the point of view previously expressed that they are likely to represent tracking errors. When many MTs begin and end in one region, as happens at the edges of the zone of overlap, it is not surprising that a few tubules should begin and end within a section thickness along the spindle axis and nearer than one MT diameter in the transverse plane. Such ends and beginnings would of course be identified as "continuous" MTs in our analysis. The complete absence of continuous MTs from metaphase spindles of *Fragilaria* is consistent with this explanation for their occurrence (37).

The decrease and subsequent increase in total tubule length during mitosis would seem to imply a complicated set of changes in the MT assembly equilibrium. This need not be the case, however, for we are looking here only at the central spindle. There are peripheral MTs that shorten during anaphase (data not shown), and their subunits may be cycled into the central spindle at constant or even decreasing assembly equilibrium to make the long polar MTs elongate. In addition, the increase in total tubule length seen in telophase

may be exaggerated on account of the possibility of thinner sections in that spindle.

One can question the validity of making statements on the shifts in microtubule length or polymer equilibrium from a sample of six cells. Our concern over the small sample size has, to some extent, been reduced by the observation that each relationship between cells which we have studied has shown consistent trends, rather than sharp fluctuations. The total number of MTs drops consistently from prometaphase to anaphase. The average lengths of both the short and the long tubules change consistently, albeit in opposite directions. The extent of overlap and the total amount of polymer in the initial spindle change first in one direction and then the other, but they show a smooth pattern of variation. Thus, while our sample size is small we are encouraged by the internal consistency of the data to believe in its quality and in the acceptability of making comparisons between different *Diatoma* spindles.

A major limitation of this study is the lack of analysis of kinetochore MTs. This is unavoidable with *Diatoma* where the cell seems to lack such MTs, at least after prometaphase. Pickett-Heaps is currently analyzing the behavior of kinetochores in diatoms by light and electron microscopy, but little is yet known of their behavior. Our future plans include a three-dimensional reconstruction study of an organism possessing well-defined kinetochores so we can look at the relationships between polar and kinetochore tubules. Interactions between polar MTs from opposite poles are the subject of the following paper (15).

This work was supported by a National Science Foundation grant (PCM 77-14796) to J. Richard McIntosh.

*Received for publication 11 January 1979, and in revised form 29 May 1979.*

## REFERENCES

1. ALLEN, C., AND G. G. BORISY. 1974. Structural polarity and directional growth of microtubules of *Chlamydomonas* flagella. *J. Mol. Biol.* **90:** 381–402.
2. BAJER, A., AND J. MOLE-BAJER. 1975. Lateral movements in the spindle and the mechanism of mitosis. *In* Molecules and Cell Movement. S. Inoué and R. E. Stephens, editors. Raven Press, New York. 77–96.
3. BAJER, A. S., AND J. MOLE-BAJER. 1972. Spindle dynamics and chromosome movements. *Int. Rev. Cytol.* **34**(Suppl. 3):1–271.
4. BRYAN, J. 1976. A quantitative analysis of microtubule elongation. *J. Cell Biol.* **71:**749–767.
5. COSS, R. A., AND J. D. PICKETT-HEAPS. 1974. The effects of isopropyl *N*-phenyl carbamate on the green alga *Oedogonium cardiacum*. I. Cell division. *J. Cell Biol.* **63:**84–98.
6. DENTLER, W. L., S. GRANETT, G. B. WITMAN, AND J. L. ROSENBAUM. 1974. Directionality of brain microtubule assembly *in vitro*. *Proc. Natl. Acad. Sci. U. S. A.* **71:**1710–1714.
7. FUGE, H. 1977. Ultrastructure of the mitotic spindle. *Int. Rev. Cytol.* **6**(Suppl):1–58.
8. HEATH, I. B. 1978. Experimental studies of mitosis in the fungi. *In* Nuclear Division in the Fungi. I. B. Heath, editor. Academic Press, Inc., New York. 89–176.
9. JOHNSON, K. A., AND G. G. BORISY. 1977. Kinetics of microtubule self-assembly *in vitro*. *J. Mol. Biol.* **117:**1–32.
10. KATZ, L., AND C. LEVINTHAL. 1972. Interactive computer graphics, and representation of complex biological structures. *Annu. Rev. Biophys. Bioeng.* **1:**465–504.
11. KUBAI, D. 1975. The evolution of the mitotic spindle. *Int. Rev. Cytol.* **43:**167–227.
12. LOPRESTI, V., E. R. MACAGNO, AND C. LEVINTHAL. 1974. Structure and development of neuronal connections in isogenic organisms: transient gap junctions between growing optic axons and lamina neuroblasts. *Proc. Natl. Acad. Sci. U. S. A.* **71:**1098–1102.
13. MARGOLIS, R. L., AND L. WILSON. 1978. Opposite end assembly and disassembly of microtubules at steady state *in vitro*. *Cell.* **13:**1–8.
14. MARGOLIS, R. L., L. WILSON, AND B. I. KIEFER. 1978. Mitotic mechanism based on intrinsic microtubule behavior. *Nature (Lond.).* **272:**450–452.
15. MCDONALD, K. L., M. K. EDWARDS, AND J. R. MCINTOSH. 1979. Cross-sectional structure of the central mitotic spindle of *Diatoma vulgare*. Evidence for specific interaction between antiparallel microtubules. *J. Cell Biol.* **83:**443–461.
16. MCDONALD, K. L., J. D. PICKETT-HEAPS, J. R. MCINTOSH AND D. H. TIPPIT. 1977. On the mechanism of anaphase spindle elongation in *Diatoma vulgare*. *J. Cell Biol.* **74:**377–388.
17. MCINTOSH, J. R. 1979. Cell division. *In* Microtubules. K. Roberts and J. S. Hyams, editors. Academic Press, Inc., London, In press.
18. MCINTOSH, J. R., J. E. SISKEN, AND L. K. CHU. 1979. Structural studies on mitotic spindles isolated from cultured human cells. *J. Ultrastruct. Res.* **66:**40–52.
19. MCINTOSH, J. R. 1977. Mitosis *in vitro*: Isolates and models of the mitotic apparatus. *In* Mitosis Facts and Questions. M. Little, N. Paweletz, C. Petzelt, H. Ponstingl, D. Schroeter, and H.-P. Zimmerman editors. Springer-Verlag, Berlin. 167–195.
20. MCINTOSH, J. R., W. Z. CANDE, E. LAZARIDES, K. MCDONALD, AND J. A. SNYDER. 1976. Fibrous elements of the mitotic spindle. *Cold Spring Harbor Conf. Cell Proliferation.* **3C:**1261–1272.
21. MCINTOSH, J. R., Z. CANDE, J. SNYDER, AND K. VANDERSLICE. 1975. Studies on the mechanism of mitosis. *Ann. N. Y. Acad. Sci.* **253:**407–427.
22. MCINTOSH, J. R., W. Z. CANDE, AND J. A. SNYDER. 1975. Structure and physiology of the mammalian mitotic spindle. *In* Molecules and Cell Movement. S. Inoué and R. E. Stephens, editors. Raven Press, New York. 31–76.
23. MURPHY, D. B., K. A. JOHNSON AND G. G. BORISY. 1977. The role of tubulin-associated proteins in microtubule nucleation and elongation. *J. Mol. Biol.* **117:**33–52.
24. OAKLEY, B. R., AND I. B. HEATH. 1978. The arrangement of microtubules in serially sectioned spindles of the alga *Cryptomonas*. *J. Cell Sci.* **31:**53–70.
25. OOSAWA, F. 1970. Size distributions of protein polymers. *J. Theor. Biol.* **27:**69–86.
26. OOSAWA, F., AND M. KASAI. 1967. A theory of linear and helical aggregations of macromolecules. *J. Mol. Biol.* **4:**10–21.
27. PEACHEY, L. D., C. H. DAMSKY, AND A. VEEN. 1975. Three-dimensional reconstruction from high-voltage electron micrographs. Proceedings of the 4th International Congress on Stereology. 207–210.
28. PETERSON, J., AND H. RIS. 1976. Electron microscopic study of the spindle and chromosome movement in the yeast *Saccharomyces cerevisiae*. *J. Cell Sci.* **22:**219–242.
29. PICKETT-HEAPS, J. D., K. L. MCDONALD, AND D. H. TIPPIT. 1975. Cell division in the pennate diatom *Diatoma vulgare*. *Protoplasma.* **86:**205–242.
30. PICKETT-HEAPS, J. D., AND D. H. TIPPIT. 1978. The diatom spindle in perspective. *Cell.* **14:**455–467.
31. RAKIC, P., L. J. STENAS, E. P. SAYRE, AND R. L. SIDMAN. 1974. Computer-aided three-dimensional reconstruction and quantitative analysis of cells from serial electron microscopic montages of foetal monkey brain. *Nature (Lond.).* **250:**31–34.
32. ROTH, L. E., D. J. PIHLAJA, AND Y. SHIGENAKA. 1970. Microtubules in the heliozoan axopodium. I. The gradion hypothesis of allosterism in structural proteins. *J. Ultrastruct. Res.* **30:**7–37.
33. SALMON, E. D. 1975. Spindle microtubules: Thermodynamics of *in vivo* assembly and role in chromosome movement. *Ann. N. Y. Acad. Sci.* **253:**383–406.
34. STEVENS, B. J. 1977. Variation in number and volume of the mitochondria in yeast according to growth conditions. A study based on serial sectioning and computer graphics reconstruction. *Biol. Cell.* **28:**37–56.
35. TILNEY, L. G. 1971. How microtubule patterns are generated: The

relative importance of nucleation and bridging of microtubules in the formation of the axonemes of *Raphidiophrys*. *J. Cell Biol.* **51**:837–854.
36. TIPPIT, D. H., AND J. D. PICKETT-HEAPS. 1977. Cell division in the pennate diatom *Surirella ovalis*. *J. Cell Biol.* **73**:705–727.
37. TIPPIT, D. H., D. SCHULZ, AND J. D. PICKETT-HEAPS. 1978. Analysis of the distribution of spindle microtubules in the diatom *Fragilaria*. *J. Cell Biol.* **79**:737–763.
38. TUCKER, J. B. 1970. Initiation and differentiation of microtubule patterns in the ciliate *Nassula*. *J. Cell Sci.* **7**:793–821.
39. WARD, S., N. THOMSON, J. G. WHITE, AND S. BRENNER. 1975. Electron microscopical reconstruction of the anterior sensory anatomy of the nematode *Caenorhabditis elegans*. *J. Comp. Neurol.* **160**:313–338.
40. WARE, R. W., AND V. LOPRESTI. 1974. Three-dimensional reconstruction from serial sections. *Int. Rev. Cytol.* **40**:325–440.